RSC Advances

ROYAL SOCIETY OF CHEMISTRY

www.rsc.org/advances

Journal Name

ARTICLE

New luminescent Cd(II)-MOF as highly selective chemical probe for Fe^{3+} in aqueous solution with mixed metal ions†

Yunlong Wu, Guo-Ping Yang*, Yingdi Zhang, Nannan Shi, Jun Han and Yao-Yu Wang*

Received 00th January 20xx,
DOI: 10.1039/x0xx00000x

www.rsc.org/

A new metal-organic framework (MOF) with the formula $[Cd(H_2L_a)_{0.5}(H_2L_b)_{0.5}(H_2O)]$ (**1**), where $H_2L_a^{2-}$ and $H_2L_b^{2-}$ represent two different coordination modes of H_2L^{2-} ligands (H_4L = [1,1':4',1"-terphenyl]-2',4,4",5'-tetracarboxylic acid), has been synthesized successfully by solvothermal reaction, and characterized by the elemental analysis, FT-IR spectroscopy, powder X-ray diffraction (PXRD), and thermogravimetric analysis (TGA). Interestingly, H_2L^{2-} adopted two coordination fashions during the self-assembled process of **1** because of the effect of partially deprotonated H_4L ligands, which resulted the 3D framework of **1** showing a trinodal (4,4,4)-connected ***PtS*** topology with a point symbol of $(4^2{\cdot}8^4)$. More mportantly, the product of **1** displays the greatly intense luminescence in solid state and high sensitivity and selectivity for Fe^{3+} ion in aqueous solution with mixed ions, making it as a new potential probe for detecting Fe^{3+}, and the quenching mechanisms were also further discussed in detail.

1. Introduction

Metal-organic frameworks (MOFs), as a new kind of molecular material, are combined by the metal ions/clusters and organic ligands via coordination bonds as well as weak intermolecular interactions[1]. MOFs have received much more attention because of its potential applications as functional materials for catalysis, gas adsorption and storage (*e.g.*, N_2, CO_2, H_2, and CH_4, *etc.*), selective separation, sensing, molecular recognition, and so on[2]. Therefore, it will be a great chance and challenge to develop new synthetic strategies from experimental and theoretical perspectives to achieve much more diverse MOFs with targeted structures and properties[3].

Very recently, luminescent metal-organic frameworks (LMOFs) are of great interests as sensing materials because of its prominent optical properties, tunable structures and relatively long emission wavelengths. To date, chemists have synthesized various LMOFs sensors in different application fields. For instance, Chen et al. have synthesized a LMOF can act as the thermometer in the range of 10-300K. Dinca's group has reported the Mg and Zn-based LCPs, showing the highly sensitivity to NH_3. And a Zn-based LCP reported by Wang *et al*. can detect H_2O reversibly by the colour and intensity change caused by hydration/depletion[4d]. Now, iron is a ubiquitous metal in cells and plays a vital role in the biological metabolism of cellular systems. Not just for the organisms, it is also, more broadly, an environmental contaminant. So, it is an urgent project to detect Fe^{3+} by an accurate way. Recent studies show that LMOFs as new optical materials can provide an effective method to detect Fe^{3+} ions[5]. On the other hand, some structural and experimental factors, such as coordination geometries of metal ions and ligands, the molar ratio of metal and ligands, role of solvents, temperature and pH et al, have been found to play key roles in the construction of MOFs[6]. Among these factors, the selection of well-designed organic linkers has a positive influence on the final functional MOFs with attractive properties and high-dimensional architectures[7]. Currently, the rigid conjugated aromatic multi-carboxylic ligands have been extensively employed as the fundamental molecular blocks to build functional MOFs due to the predictable coordination and bridging fashions as well as good stabilities[8,9].

Based on the above-mentioned factors and further complement of our previous works[10], herein, a conjugated aromatic tetracarboxylic ligand, [1,1':4',1"-terphenyl]-2',4,4",5'-tetracarboxylic acid (H_4L), has been chosen as the organic linker with d^{10} Cd(II) ions to construct crystalline solid luminescent materials. As a result, a new Cd(II)-MOF, namely $[Cd(H_2L_a)_{0.5}(H_2L_b)_{0.5}(H_2O)]$, was successfully synthesized via solvothermal reaction, in which $H_2L_a^{2-}$ and $H_2L_b^{2-}$ represent two different coordination models of H_2L^{2-} in the self-assembled process. In addition, the solid state luminescent property of **1** has also been investigated under the irradiation of ultraviolet at ambient temperature. More importantly, the product of **1** displayed highly selective to Fe^{3+} in aqueous solution with mixed metal ions due to the quenching effect, making it as a new probe for detecting Fe^{3+} ions. And the quenching mechanism of **1** has also been further studied in detail.

2. Experimental section

2.1. Materials and measurements

All starting analytical grade materials and solvents in experiments were obtained commercially and used without further purification.

[a] *Key Laboratory of Synthetic and Natural Functional Molecule Chemistry of Ministry of Education, Shaanxi Key Laboratory of Physico-Inorganic Chemistry, College of Chemistry and Materials Science, Northwest University, Xi'an 710069, P.R. China. E-mail: ygp@nwu.edu.cn; wyaoyu@nwu.edu.cn.*

† Electronic Supplementary Information (ESI) available: FT-IR, TGA, and PXRD patterns, and the additional figures of MOFs. For the ESI and crystallographic data in CIF or other electronic format. See DOI: 10.1039/b000000x/

Elemental analyses of C and H were performed on Perkin-Elmer 2400C Elemental Analyzer. IR (KBr pellet) spectra were recorded on Bruker EQUINOX-55 in the range of 4000 ~ 400 cm^{-1}. Power X-ray diffraction (PXRD) pattern was obtained on Bruker D8 ADVANCE X-ray powder diffractometer (Cu-Kα, λ = 1.5418 Å). Thermogravimetric analyses (TGA) were carried out by NETZSCH STA 449C microanalyzer thermal analyzer in N_2 atmosphere with a heating rate of 10 °C min^{-1}. The solid state luminescent spectra were performed on Hitachi F4500 fluorescence spectrophotometer at ambient temperature. UV-Vis spectrums were detected on Hitachi U-3310 spectrometer. Inductively coupled plasma (ICP) experiments were conducted on IRIS Advantage spectrometer.

2.2. Synthesis of $[Cd(H_2L_a)_{0.5}(H_2L_b)_{0.5}(H_2O)]$ (1)

A mixture of $Cd(NO_3)_2{\cdot}6H_2O$ (0.1 mmol, 30.8 mg), H_4L (0.05 mmol, 20.3 mg) and 10 mL H_2O/N-methyl-2-pyrrolidone (NMP) (3/7) were mixed in 15 mL Teflon-lined stainless steel vessel, which were heated at 145 °C for 72 h and then cooled to the room temperature at the rate of 10 °C h^{-1} to form colourless block crystals. Yield 48% (based on H_4L). Elemental analysis of **1**, calculated (%): C 49.41, H, 2.64; found: C 49.53, H 2.59. FT-IR (KBr, cm^{-1}) (Fig. S1, ESI†): 3410 (m), 2925 (w), 1679 (s), 1542 (s), 1420 (s), 1263 (s), 870 (m), 763 (m), 583 (w), 513 (w).

2.3. Crystal structure determination

The diffraction data were collected on a Bruker SMART APEXII CCD diffractometer equipped with graphite-monochromated Mo-Kα radiation (λ = 0.71073 Å) at 298K. The structures were solved by direct methods and refined by a full-matrix, least-squares refinement based on F^2 with SHELXL-97[11]. All non-hydrogen atoms were refined anisotropically with the hydrogen atoms were calculated and assigned their ideal positions with isotropic displacement factors and included in the final refinement by use of geometric restraints. The relevant crystallographic data are summarized in Table 1. Selected bond lengths and angles are listed in Table S1 (ESI†). CCDC number is 1415768 for **1**.

Table 1. Crystal data and structure refinements for **1**

Complex	1
Empirical formula	$C_{22}H_{14}CdO_9$
Formula mass	534.73
Crystal system	Triclinic
Space group	*P*-1
a [Å]	4.9361(9)
b [Å]	12.949(2)
c [Å]	15.145(3)
α [°]	90.758(3)
β [°]	96.573(3)
γ [°]	92.174(3)
V [Å^3]	960.8(3)
Z	2
D_{calcd} [g·cm^{-3}]	1.848
μ [mm^{-1}]	1.194
F [000]	532
θ [°]	1.35-24.99
Reflections collected	4730 / 3300
Goodness-of-fit on F^2	1.061
Final $R^{[a]}$ indices [I>2σ(I)]	R_1 = 0.0603, wR_2 = 0.1750

[a] $R_1=\sum||F_o|-|F_c||/\sum|F_o|$, $wR_2=[\sum w(F_o^2-F_c^2)^2/\sum w(F_o^2)^2]^{1/2}$

3. Results and discussion

3.1. Structure description of $[Cd(H_2L_a)_{0.5}(H_2L_b)_{0.5}(H_2O)]$

Single-crystal X-ray analysis shows that **1** crystallizes in the triclinic crystal system with *P-1* space group. The asymmetric unit consists of two kinds of partially deprotonated H_2L^{2-} ligands ($H_2L_a^{2-}$ and $H_2L_b^{2-}$), adopting different coordination models with Cd(II) ions (Scheme 1). As shown in Fig. 1, the Cd(II) ion is located in the centre of the distorted octahedral coordination geometry, which is coordinated with three oxygen atoms from two carboxylate groups belonging to two $H_2L_a^{2-}$ ligands, two oxygen atoms from two $H_2L_b^{2-}$ ligands and water molecule, respectively. The Cd-O bond lengths [2.201(5) ~ 2.446(6) Å] and Cd-O-Cd angles [53.9(2)° ~ 169.1(2)°] are in the normal range of reported Cd(II)-carboxylate MOFs[12].

In **1**, the most interesting structural feature is that the partially deprotonated H_2L^{2-} ligands adopt two different coordination modes ($H_2L_a^{2-}$ and $H_2L_b^{2-}$) to extend the framework of **1**. In $H_2L_a^{2-}$ tecton, the four carboxylate groups display two different fashions: ($\eta^2\mu_1\chi^2$) bidentate and ($\eta^1\mu_1\chi^1$) monodentate, producing an infinite $1D_a$ chain along *b* axis (Fig. 2a). As for $H_2L_b^{2-}$ ligand, the carboxylate groups show one bridging bidentate connection fashion ($\eta^2\mu_2\chi^2$) to generate another $1D_b$ chain along *a* axis and the other two carboxylic groups are not involved in coordination process (Fig. 2b), which further bridge the $1D_a$ chains to give a 3D framework (Fig. 2c and S2, ESI†). Topologically, the Cd(II) ions, $H_2L_a^{2-}$ and $H_2L_b^{2-}$ ligands are all considered as four-connected nodes (Fig. S3, ESI†), thus, the whole framework of **1** can be simplified as a trinodal (4,4,4)-connected ***PtS*** topology with a point symbol of ($4^2{\cdot}8^4$) (Fig. 2d).

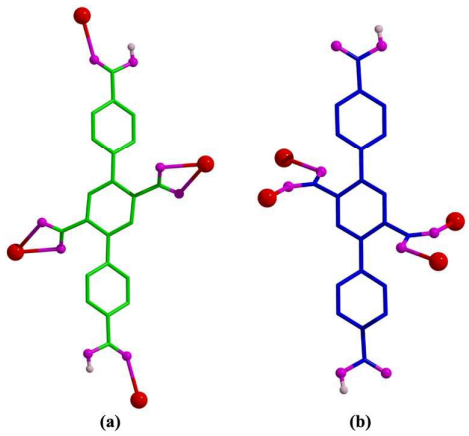

Scheme 1 Various coordination models of H_2L^{2-} ligands (a: $H_2L_a^{2-}$; b: $H_2L_b^{2-}$) with Cd(II) ions.

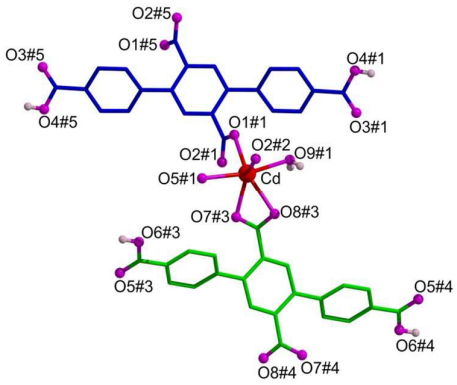

Fig. 1 Coordination environment of center Cd(II) ions. Symmetry codes: #1: x, y, z; #2: 1+x, y, z; #3: 2-x, -y, 1-z; #4: x, 1+y, z; #5:1-x, -y, 2-z.

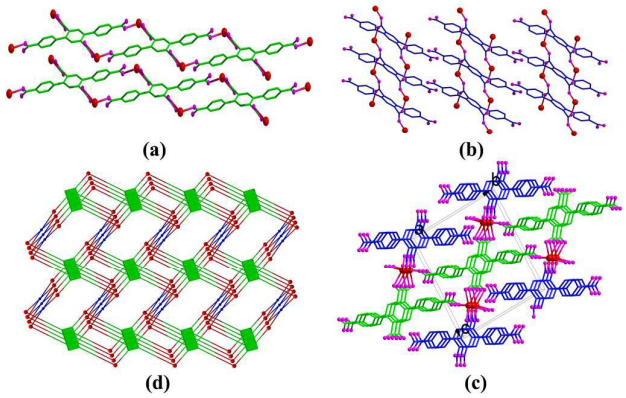

Fig. 2 (a) Structure of $1D_a$ chains generated by $H_2L_a^{2-}$ ligand viewed along *b* axis. (b) Structure of $1D_b$ chains generated by $H_2L_b^{2-}$ ligand viewed along *a* axis. (c) 3D framework of **1**. (d) Topological net of **1**.

3.2. PXRD and TGA

The phase purity of the bulk materials was confirmed by the good matches between the experimental PXRD pattern and the simulated pattern from the single-crystal data of **1** (Fig. S4, ESI†). Also, to estimate the thermal stability of the product, the thermogravimetric analyses (TGA) of **1** was conducted in N_2 atmosphere (Fig. S5, ESI†). The TGA curve shows that **1** releases one coordinate water molecule below ~140 °C with a total weight loss of 4.0% (calcd 3.4%). And the structure keeps relatively stable in the range of 140-400 °C and then collapses. Most importantly, the product of **1** is very stable in the aqueous solution for almost one month.

3.3. Photoluminescence properties

More recently, MOFs with d^{10} metal ions have been attracted much attention because of their potential photoluminescent properties and potentials as optical materials and chemical sensors[11]. Thus, the solid state luminescent properties of H_4L ligand and **1** have been tested at room temperature. Upon excitation at 280 nm for H_4L and 330 nm for **1**, the maximum emission peaks were observed at 414 and 385 nm, respectively (Fig. 3). The blue shift of **1** compared with the H_4L ligand can be assigned to ligand-centred emission (π-π^* and/or n-π^* transition)[14]. Moreover, because of the good stability and the visible blue light of **1** excited by the ultraviolet light, the products of **1** was selected as the chemical recognition material to detecting different metal ions in aqueous solution.

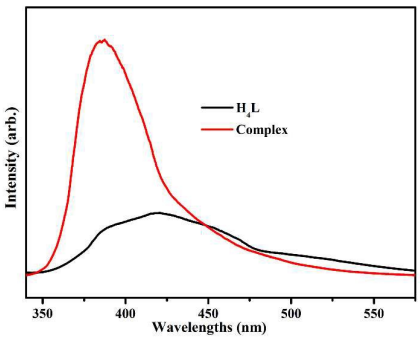

Fig. 3 Solid-state luminescent emission spectra of H_4L and **1**.

In order to explore the sensing properties of **1**, the as-synthesized products were grinded (3 mg) and immersed in the aqueous solution (3 mL) contained 0.01 mol L^{-1} $M(NO_3)_n$ (M = Cd^{2+}, H_2O, Mg^{2+}, Li^+, K^+, Na^+, Zn^{2+}, Mn^{2+}, Ca^{2+}, Hg^{2+}, Pb^{2+}, Al^{3+}, Ni^{2+}, Cu^{2+}, Co^{2+}, Fe^{3+}) for 24 hours. As displayed in Fig. 4a and S6, ESI†, the luminescent properties show the different intensities depending on the nature of metal ions, especially for Fe^{3+}, exhibiting the significant quenching effect, and the visible colour changes have also been recorded (Fig. S7, ESI†). Furthermore, the selective sensing properties have been explored carefully (Fig. S8, ESI†). And there exists a relatively strong luminescent intensity of **1** in the aqueous solution with the various metal ions without Fe^{3+}, however, the luminescence was completely quenched immediately by the addition of Fe^{3+} into the system, indicating the high selective sensing for Fe^{3+} ion.

The exploration of the relationship between the luminescent intensities and the concentration was carried out by changing Fe^{3+} ions concentration from 10^{-5} ~ 10^{-4} M (Fig. 4b). The luminescent intensity of **1** is quenched completely at the concentration of Fe^{3+} up to 10^{-4} M, and the detection limitation of 10^{-5} M for **1** is a relatively lower value in comparison with those of the reported sensors for sensing Fe^{3+} ions[15]. And the relationship between the luminescent intensities and the concentration of Fe^{3+} ions can be fitted well with the linear equation, as shown in the up inset of Fig. 4b: I/I_0 = -10.6 $[Fe^{3+}]$ + 0.94 (R^2 = 0.98965), where the *I* and I_0 are the luminescent intensities of solution with different concentration of Fe^{3+} ions and blank sample. The result shows that the decrease of the luminescent intensities was dependent on the addition of the concentration of Fe^{3+}, illustrating the diffusion-controlled quenching process for Fe^{3+} ion[16].

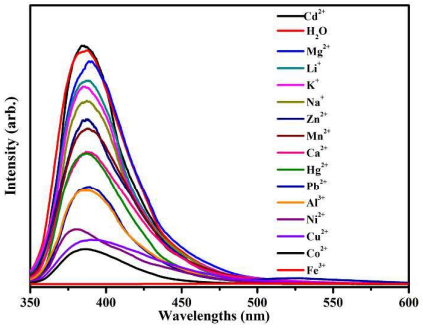

(a)

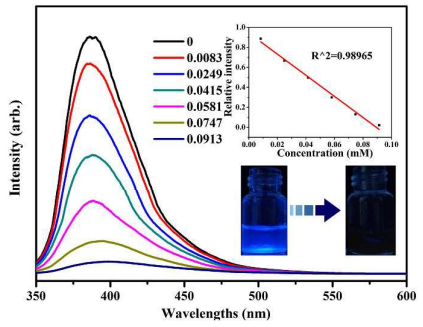

(b)

Fig. 4 (a) Emission spectra of **1** in aqueous solution containing various metal ions. (b) Luminescent emission spectra of **1** in aqueous solution containing different concentration of Fe^{3+} ions, the insets display the relationship between the concentration and luminescent intensity (top), and show the colour change of the solution (below).

3.4. Possible quenching mechanism of luminescence

The latest reported LMOFs used as sensing materials reveal that the quenching mechanisms are closely related to the structures of the LMOFs. The tunable structures and permanent porosity of LMOFs make them become the excellent candidates for capturing of analytes in the pores, which allow them to be in close proximity with the organic walls or the metal centers of the host motif, and thus readily interact with LMOFs and suitable for using as fluorescence sensors. The major reason is that the accessible channels and functional sites (Lewis basic/acidic sites and open metal sites) produce their high selective recognition for the analytes. And the interactions between the frameworks and analytes can give rise to a lower detection limit and higher sensing sensitivity. In addition, some LMOFs have even been used as fluorescent for metal ions via cation-exchange[17].

In order to evaluate the possible mechanism for luminescent quenching by Fe^{3+}, the following series of experiments have been well conducted. Firstly, the PXRD patterns of the products match well with the simulated pattern from single-crystal data after series of sensing experiments (Fig. S9, ESI†), showing that **1** can keep its original framework and be reused in the sensing studies. And the inductively coupled plasma (ICP) experiments have also been carried out to check the stability of **1** after the sensing experiments (Fig. S10, ESI†), revealing that there is no release of Cd^{2+} ion in the sensing process and the structure of **1** is stable in the aqueous solution. Moreover, the UV-Vis absorption spectra of the aqueous solution with various metal ions have also been studied (Fig. 5). Due to the maximum excitation peak of **1** is ~330 nm, the metal ions will lead to the strong quenching effect on the luminescent intensity of **1**, if there is a high UV-Vis absorbance in this range. The results show that only the Fe^{3+} ions have a stronger absorbance at 280 ~ 330 nm in comparison with other metal ions, explaining the sole sensitivity to the luminescence of the above system[18]. More importantly, the structure analysis display that there exist the uncoordinated oxygen atoms in **1**, herein, the quenching mechanism could be explained by donor-acceptor electron transfer. When the Fe^{3+} ions incorporated with the **1** in the aqueous solution and excited by ultraviolet light, the uncoordinated oxygen atoms of **1**, acting as the electrons donor, donate its electrons to Fe^{3+} ions (the electrons acceptor) to form an electron-deficient region, resulting in the energy migration and luminescent quenching[19].

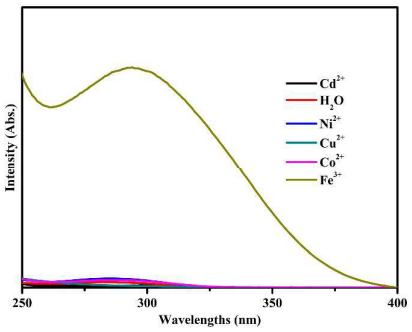

Fig. 5 UV-Vis absorption spectra of different metal ions.

Conclusion

In summary, a new Cd(II)-MOF has been yielded successfully via solvothermal reaction. The structural analysis indicated that the partially deprotonated H_2L^{2-} took two coordination modes and had a positive influence on the assembled process of **1**. The product of **1** has remarkable water stability and displays the highly selective detection of Fe^{3+} in aqueous solution with mixed metal ions, suggesting that it can act as a new potential luminescent sensor for Fe^{3+} ions. More importantly, **1** can keep its original framework and be reused after the series of sensing experiments in the studies. The results have a great signification in developing the applicable scope of LMOFs. It is anticipated that much more future efforts should be devoted not only in the design and synthesis of various LMOFs to detect metal ions in the aqueous solution but also to further explore the promising biocompatibility in the sensing areas of the medical diagnostics, and cell biology, *etc*.

Acknowledgements

This work was supported by the NSFC (Grants 21201139, 21371142, and 21531007), NSF of Shaanxi Province (Grant 2013JQ2016), and the Open Foundation of Key Laboratory of Synthetic and Natural Functional Molecule Chemistry of Ministry of Education (Grant 338080049).

Notes and references

1 (a) J. R. Long and O. M. Yaghi, *Chem. Soc. Rev.*, 2009, **38**, 1213; (b) H.-C. Zhou, J. R. Long and O. M. Yaghi, *Chem. Rev.*, 2012, 112, 673; (c) We. Lu, Z. Wei, Z.-Y. Gu, T.-F. Liu, J. Park, J. Park, J. Tian, M. Z, Q. Zhang, T. Gentle III, M. Bosch and H.-C. Zhou, *Chem. Soc. Rev.*, 2014, **43**, 5561; (d) D.-Y. Du, J.-S. Qin, S.-L. Li, Z.-M. Su and Y.-Q. Lan, *Chem. Soc. Rev.*, 2014, **43**, 4615; (e) N. C. Burtch, H. Jasuja, D. Dubbeldam and K. S. Walton, *J. Am. Chem. Soc.*, 2013, **135**, 7172.

2 (a) J.-P. Zhang, Y.-B. Zhang, J.-B. Lin and X.-M. Chen, *Chem. Rev.*, 2012, **112**, 1001; (b) M. L. Aubrey, R. Ameloot, B. M. Wiers and J. R. Long, *Energy Environ. Sci.*, 2014, **7**, 667; (c) L.-M. Yang, P. Ravindran and M. Tilset, *Inorg. Chem.*, 2013, **52**, 4217; (d) P. Canepa, C. A. Arter, E. M. Conwill, D. H. Johnson, B. A. Shoemaker, K. Soliman and T. Thonhauser, *J. Mater. Chem. A.*, 2013, **1**, 13597; (e) L.-M. Yang, G.-Y. Fang, J. Ma, E. Ganz and S. S. Han, *Cryst. Growth Des.*, 2014, **14**, 2532; (f) X. Zheng, L. Zhou, Y. Huang, C. Wang, J. Duan, L. Wen, Z. Tian and D. Li, *J. Mater. Chem. A.*, 2014, **2**, 12413. (g) L.-M. Yang, P. Ravindran,P. Vajeeston and M. Tilset, *Phys. Chem. Chem. Phys.*, 2012, **14**, 4713; (h) D. E. Williams, J. A. Rietman, J. M. Maier, R. Tan, A. B. Greytak, M. D. Smith, J. A. Krause and N. B. Shustova, *J. Am. Chem. Soc.*, 2014, **136**, 11886.

3 (a) M. D. Allendorf, C. A. Bauer, R. K. Bhakta and R. J. T. Houk, *Chem. Soc. Rev.*, 2009, **38**, 1330; (b) L.-M. Yang, E. Ganz, S. Svelle and M. Tilset, *J. Mater. Chem. C*, 2014, **2**, 7111; (c) F. -X. Coudert, A. H. Fuchs, *Coord. Chem. Rev.*, 2015, doi: 10.1016/j.ccr.2015.08.001; (d) L.-M. Yang,P. Vajeeston, P. Ravindran, H. Fjellvag and M. Tilset , *Inorg. Chem.*, 2010, **49**, 10283.

4 (a) M. J. Katz, T. Ramnial, H. Z. Yu and D. B. Leznoff, *J. Am. Chem. Soc.*, 2008, **130**, 10662; (b) J. J. Perry IV, J. A. Perman and M. J. Zaworotko, Chem. Soc. Rev., 2009, 38, 1400; (c) N. B.Shustova, A. F. Cozzolino, S. Reineke, M. Baldo and M. Dinca, *J. Am. Chem. Soc.*, 2013, **135**, 13326; (d) C. C. Wang, C. C. Yang, W. C. Chung, G. H. Lee, M. L. Ho, Y. C. Yu, M. W. Chung, H. S. Sheu, C. H. Shih, K. Y. Cheng, P. J. Chang and P.-T. Chou, *Chem. Eur. J.*, 2011, **17**, 9232; (f) Y. Cui, H. Xu, Y. Yue, Z. Guo, J. Yu, Z. Chen, J. Gao, Y. Yang, G. Qian and B. Chen, *J. Am. Chem. Soc.*, 2012, **134**, 3979.

5 (a) Z. Chen,Y. Sun, L. Zhang, D. Sun, F. Liu, Q. Meng, R. Wang and D. Sun， *Chem. Commun.*, 2013, **49**, 11557; (b) Y. Zhou, H.-H. Chen and B. Yan, *J. Mater. Chem. A*, 2014, **2**, 13691; (c) X.-Y. Dong, R. Wang, J.-Z.

Wang, S.-Q. Zang and T. C. W. Mak, *J. Mater. Chem. A*, 2015, **3**, 641; (d) Q. Tang, S. Liu, Y. Liu, J. Miao, S. Li, L. Zhang, Z. Shi and Z. Zheng, *Inorg. Chem.*, 2013, **52**, 2799.

6 (a) G.-P. Yang, L. Hou, L.-F. Ma and Y.-Y. Wang, *CrystEngComm*, 2013, **15**, 2561; (b) Y.-F. Hsu, W. Hsu, C.-J. Wu, P.-C. Cheng, C.-W. Yeh, W.-J. Chang, J.-D. Chen and J.-C. Wang, *CrystEngComm*, 2010, **12**, 702; (c) C.-P. Li and M. Du, *Chem. Commun.*, 2011, **47**, 5958; (d) S.-H. Zhang, L.-F. Ma, H.-H. Zou, Y. G. Wang, H. Liang and M. H. Zeng, *Dalton Trans.*, 2011, **40**, 11402; (e) J.-X. Yang, Y.-Y. Qin, J.-K. Cheng, X. Zhang and Y.-G. Yao, *Cryst. Growth Des.*, 2015, **15**, 2223; (f) L.-M. Yang, P. Ravindran, P. Vajeeston and M. Tilset, *RSC Adv.*, 2012, **2**, 1618.

7 (a) S. Durot, J. Taesch and V. Heitz, *Chem. Rev.*, 2014, **114**, 8542; (b) K. K. Bisht, Y. Rachuri, B. Parmara and E. Suresh, *RSC Adv.*, 2014, **4**, 7352; (c) Z. Zhang and M. J. Zaworotko, *Chem. Soc. Rev.*, 2014, **43**, 5444; (d) M. Ahmad, R. Katoch, A. Garg and P. K. Bharadwaj, *CrystEngComm*, 2014, **16**, 4766; (e) M. Yoshizawa and J. K. Klosterman, *Chem. Soc. Rev.*, 2014, **43**, 1885.

8 (a) H. Li, Z. Xu, B. Zhao, Y. Jia, R. Ding, H. Hou and Y. Fan, *CrystEngComm*, 2014, **16**, 2470; (b) Z.-X. Li, Y. Xu, Y. Zuo, L. Li, Q. Pan, T.-L. Hu and X.-H. Bu, *Cryst. Growth Des.*, 2009, **9**, 3904; (c) T. Muller and S. Brase, *RSC Adv.*, 2014, **4**, 6886; (d) Y. Song, X. Yin, B. Tu, Q. Pang, H. Li, X. Ren, B. Wang and Q. Li, *CrystEngComm*, 2014, **16**, 3082.

9 (a) R. D. Kennedy, D. J. Clingerman, W. Morris, C. E. Wilmer, A. A. Sarjeant, C. L. Stern, M. O ' Keeffe, R. Q. Snurr, J. T. Hupp, O. K. Farha and C. A. Mirkin, *Cryst. Growth Des.*, 2014, **14**, 1324; (b) W. Bury, D. Fairen-Jimenez, M. B. Lalonde, R. Q. Snurr, O. K. Farha and J. T. Hupp, *Chem. Mater.*, 2013, **25**, 739; (c) I. Spanopoulos, P. Xydias, C. D. Malliakas and P. N. Trikalitis, *Inorg. Chem.*, 2013, **52**, 855; (d) B. A. Blight, R. Guillet-Nicolas, F. Kleitz, R.-Y. Wang and S. Wang, *Inorg. Chem.*, 2013, **52**, 1673.

10 (a) Y. Wu, G.-P. Yang, Y. Zhao, W.-P. Wu, B. Liu and Y.-Y. Wang, *Dalton Trans.*, 2015, **44**, 3271; (b) X. Zhou, P. Liu, W.-H. Huang, M. Kang, Y.-Y. Wang and Q.-Z. Shi, *CrystEngComm*, 2013, **15**, 8125.

11 G. M. Sheldrick, SHELXL-97, *Program for Refinement of Crystal Structures*, University of Göttingen, Germany, 1997.

12 (a) C. A. Bauer, S. C. Jones, T. L. Kinnibrugh, P. Tongwa, R. A. Farrell, A. Vakil, T. V. Timofeeva, V. N. Khrustalev and M. Allendorf, *Dalton Trans.*, 2014, **43**, 2925; (b) A. V. Kuttatheyil, M. Handke, J. Bergmann, D. Lässig, J. Lincke, J. Haase, M. Bertmer and H. Krautscheid, *Chem. Eur. J.*,2015, **21**, 1118; (c) P. Rajakannu, R. Howlader, A. C. Kalita, R. J. Butcher and R. Murugavel, *Inorg. Chem. Front.*, 2015, **2**, 55; (d) N. S. and G. Anantharaman, *CrystEngComm*, 2014, **16**, 6203.

13 (a) J. Ye, L. Zhao, R. F. Bogale, Y. Gao, X. Wang, X. Qian, S. Guo, J. Zhao and G. Ning, *Chem. Eur. J.*, 2015, **21**, 2029; (b) X.-N. Zhang, L. Liu, Z.-B. Han, M.-L. Gao and D.-Q. Yuan, *RSC Adv.*, 2015, **5**, 10119.

14 (a) X. Cao, B. Mu and R. Huang, *CrystEngComm*, 2014, **16**, 5093; (b) P. Manna, B. K. Tripuramallu and S. K. Das, *Cryst. Growth Des.*, 2014, **14**, 278; (b) L. Croitor, E. B. Coropceanu, A. E. Masunov, H. J. Rivera-Jacquez, A. V. Siminel, V. I. Zelentsov, T. Y. Datsko and M. S. Fonari, *Cryst. Growth Des.*, 2014, **14**, 3935; (c) B. Mohapatra, V. Venkatesh and S. Verma, *Cryst. Growth Des.*, 2014, **14**, 5042; (d) S. Parshamoni, H. S. Jena, S. Sanda and S. Konar, *Inorg. Chem. Front.*, 2014, **1**, 611.

15 (a) Z. Xiang, C. Fang, S. Leng and D. Cao, *J. Mater. Chem. A*, 2014, **2**, 7662; (b) W. Sun, J. Wang, G. Zhang and Z. Liu, *RSC Adv.*, 2014, **4**, 55252.

16 (a) B. Chen, Y. Yang, F. Zapata, G. Lin, G. Qian and E. B. Lobkovsky, *Adv. Mater.*, 2007, **19**, 1693; (b) S. Dang, X. Min, W. Yang, F.-Y. Yi, H. You and Z.-M. Sun, *Chem. Eur. J.*, 2013, **19**, 17172; (c) G.-Y. Wang, L.-L. Yang, Y. Li, H. Song, W.-J. Ruan, Z. Chang and X.-H. Bu, *Dalton Trans.*, 2013, **42**, 12865.

17 (a) Y. Cui, Y. Yue, G. Qian and B. Chen, *Chem. Rev.*, 2012, **112**, 1126; (b) Y.-P. Zhu, T.-Y. Ma, T.-Z. Ren and Z.-Y. Yuan, *Appl. Mater. Interfaces*, 2014, **6**, 16344; (c) C.-X. Yang, H.-B. Ren and X.-P. Yan, *Anal. Chem.*, 2013, **85**, 7441.

18 H. Xu, F. Liu, Y. Cui, B. Chen and G. Qian, *Chem. Commun.*, 2011, **47**, 3153.

19 (a) S. J. Toal and W. C. Trogler, *J. Mater. Chem.*, 2006, **16**, 2871; (b) S. Pramanik, C. Zheng, X. Zhang, T. J. Emge and J. Li, *J. Am. Chem. Soc.*, 2011, **133**, 4153.